Effect of Initial Water Content on Foaming Quality and Mechanical Properties of Plant Fiber Porous Cushioning Materials

Yuying Luo, Shengling Xiao,* and Shilei Li

A porous, wood-fiber-based cushioning material for packaging was prepared in this study using poplar fiber and wood powder raw materials as an environmentally friendly resource. Water, the foaming agent azodicarbonamide and sodium bicarbonate, starch, and nucleating agent French chalk were used as additives, and the ingredients were subjected to hot-press molding. The effects of the initial water content on the foaming quality and mechanical properties of the plant fiber porous cushioning materials were explored. The results showed that the initial water content had a substantial influence on the foaming quality and mechanical properties of plant fiber porous buffer materials. When the initial water content was 69.3%, the initial embryo viscosity was the most suitable for bubble growth, and the porosity, pore size, and distribution of the samples were optimal. Furthermore, the mechanical properties of the samples were the strongest. The foaming mechanism of the plant fiber porous cushioning material was similar to the foaming mechanism of a polymer foaming material. Thus, the embryo viscosity had the greatest influence on the bubble growth process.

Keywords: Cushioning package; Initial water content; Foaming qualities; Mechanical properties

*Contact information: College of Engineering and Technology, Northeast Forestry University, 26 Hexing Road, Harbin 150040, China; *Corresponding author: shenglingxiao@126.com*

INTRODUCTION

Driven by its environmental friendliness, low cost, and unlimited market potential, interest has recently arisen in the development of plant fiber porous cushioning materials. In recent years, numerous studies have made a great breakthrough in the development of plant fiber porous cushioning materials (Li *et al.* 2013; Zeng *et al.* 2013; Ji *et al.* 2015). The materials have good mechanical properties, and they can be used in the field of cushioning packaging to replace expanded polyethylene (EPE) and expanded polystyrene (EPS) (She 2007; Wang *et al.* 2012; Huang *et al.* 2014).

However, most of the previous studies have focused on the effects of the addition of the component amounts, such as plant fiber and foaming agent, on the mechanical properties of the materials (Lawton *et al.* 2004; Carr *et al.* 2006; Wang *et al.* 2009; Cao 2013) and the influence of the molding process and parameters on the mechanical properties of the materials (Chang and Hung 2003; Chen *et al.* 2011; Zhao *et al.* 2012). The term "embryo viscosity" is used in this paper to denote the viscosity of the mixture during any expansion or other changes, and "initial embryo viscosity" is used to denote the viscosity of the mixture prior to foaming. Few studies of the effect of the embryo viscosity on the foaming process and mechanical properties of the materials have been conducted. According to the classical theory of foam molding, the foaming process is

usually divided into 4 stages: the formation of a gas solution, the nucleation of bubbles, the bubble growth, and the stabilization of bubbles. The embryo viscosity directly affects the nucleation and growth stages of bubbles. Too high an embryo viscosity can lead to a low foam ratio, and too low of embryo viscosity can lead to the material overflow, the consolidation, collapse, or rupture of the bubble holes, and other defects. These affect the porosity and pore structure parameters of the material, and the structure of the bubble has a direct influence on the mechanical properties of the material (Wang 2012). Therefore, proper embryos viscosity is the key factor to obtain porous buffer materials with good mechanical properties and pore structure.

In this paper, wood fiber porous materials were prepared using poplar fiber and wood powder as raw materials and using water, a foaming agent, starch, and a nucleating agent as additives. The viscosity of the embryo could not be measured, because it does not have mobility. Therefore, the initial water content of the embryo was used to characterize the degree of stickiness. When the initial water content was high, the viscosity of the embryo was small. An image processing software called Image Pro Plus 6.0 was used to analyze the micro images of materials and the bubble parameters of the different samples were determined. Static compression tests were performed to measure the mechanical properties of the samples. The effect of the initial water content, *i.e.*, the embryo viscosity, on the foaming and mechanical properties of the material was investigated. The results of this study revealed the foam mechanism of wood fiber porous cushioning material, providing theoretical support for further research.

EXPERIMENTAL

Materials

Poplar wood powder and poplar wood pulp were obtained from the Baihe Forestry Bureau of Jilin (Baihe, China) and the Bioenergy Laboratory of Northeast Forestry University, Harbin, China, respectively. The azodicarbonamide, zinc oxide, French chalk, and sodium bicarbonate were purchased from Tianjin Xinbote Chemical Co., Ltd. (Tianjin, China). The polyvinyl alcohol (PVA) and pregelatinized starch were obtained from the Shanxi Sanwei Group Co., Ltd. (Hongtong, China) and Heilongjiang Songtian Potato Industry Co., Ltd. (Suihua, China), respectively.

The ZG-20T precision automatic tablet press was produced by Dongguan Zengoon Electromechanical Equipment Technology Co., Ltd. (Dongguan, China). The electric thermostatic water bath and the 101-3A type electric heating air blast drying box were produced by Tianjin Taisite Instrument Co., Ltd. (Tianjin, China). The ZT16-00 standard fiber dissociation device and the ZT17-00 pulp beating degree instrument were produced by Xingping Zhongtong Test Equipment Co., Ltd. (Xingping, China). The YDN-15 computer control compression test instrument was produced by Changchun Yueming Small Testing Machine Co., Ltd. (Changchun, China).

Methods

Mixing of components

First, 20 g of wood powder, 3 g of pregelatinized starch, 3 g of foaming agent, and 5 g of talcum powder were mixed and stirred to make a uniform, dry mixture. Meanwhile, the wood pulp with different water contents, 45 g of PVA aqueous solution, and 10 g of glycerin was mixed by a blender for 5 min to make a uniform wet mixture.

Then, the dry mixture was added into the wet mixture and stirred until it reached a uniform consistency. Finally, a uniform mixture of materials was obtained by adding 0.1 g of borax and stirring for 10 min to make the mixture cross-linking even.

Molding process

To achieve a good foaming effect, a subsection hot pressing method was used. First, the mixture was placed in a mold that was pre-covered with a release agent called polytetrafluoroethylene. Then, the temperature of the first stage was set under the boiling point, which was 90 °C and remained at that temperature for 30 min. The temperature of the second stage was 165 °C, and remained at that temperature for 40 min. Finally, the sample was cooled down and de-molded using the refrigeration system of the precision automatic tablet press, and it was dried by electric heating in an air blast drying box. During this process, the pressure of the press was 0 MPa, because the press plate played the role of the mold.

The porous buffer materials with different initial water contents were prepared using different amounts of water. Three replicates were performed for each group. The amount of water and initial water content of the different samples are shown in Table 1.

Table 1. Amount of Water and Initial Water Content of Different Samples

Amount of Water (g)	96	100	104	108	112	116	120	124
Initial Water Content (%)	66.9	67.6	68.2	68.8	69.3	69.9	70.4	70.9

Characterization of foaming quality

The foaming quality of the materials usually has been characterized by the porosity, average diameter of the cell, and standard deviation of the cell diameter distribution (Hong *et al*. 2011). Porosity refers to the ratio of the volume of pores in the material to the total volume of the material. It is one of the most basic parameters of porous materials, and determines the physical properties and mechanical properties of porous materials. In this paper, the equivalent porosity was used, that was, the ratio of the area occupied by the pores in the image to the whole area of the image. The stereomicroscope (Saike Digital Technology Development Co. Ltd., Shenzhen, China) was used to observe and photograph the transverse and longitudinal sections of different samples under the same magnification. Microscopic images were processed and analyzed by a professional image analysis software called Image Pro Plus 6.0 (Media Cybernetics, Bethesda, USA). Then the porosity and cell average diameter of the samples were obtained. The cell diameter fluctuation was characterized by standard deviation. The cell diameter standard deviation was calculated according to Eq. 1,

$$S_d = \sqrt{\frac{1}{n}\sum_{i}^{n}(D_i - \overline{D})^2} \quad (1)$$

where S_d is the cell diameter standard deviation, D_i is the diameter of every cell (μm), and D is the cell average diameter (μm).

Static compression properties

The static compression properties were measured according to the Chinese National Standard GB/T 8168-2008 (2008), Method A, which is the static compression test method for buffer package materials. In the experiment, the load applied to the

samples was gradually increased at a speed of 12 mm/min ± 3 mm/min. The load and displacement of the samples were recorded in the process of compression, and the original load-displacement (*F*-*s*) curves were obtained. To eliminate the influence of material thickness, the *F*-*s* curve was converted into the stress-strain (*σ*-*ε*) curve according to Eqs. 2 and 3,

$$\sigma = \frac{P}{A} \times 10^6 \quad (2)$$

where σ is the compression force (Pa), P is the load (N), and A is the loading area (mm^2).

$$\varepsilon = \frac{T - T_i}{T} \quad (3)$$

In Eq. 3, ε is the compressive strain, T is the thickness of the sample before compression (mm), and T_i is the thickness of the sample after compression (mm).

The buffer coefficient was calculated according to Eqs. 4 and 5 (Fang 2013),

$$E = \int_0 \sigma \, d\varepsilon \quad (4)$$

$$C = \frac{\sigma}{E} \quad (5)$$

where E is the deformation energy per unit volume ($J \cdot cm^{-3}$), and C is the buffer coefficient.

Four-time compression resilience

The sample was compressed at a speed of 12 mm/min ± 3 mm/min until it was compressed to half of the original thickness. Then, the sample was unloaded and remained for one minute to measure the thickness of specimen. Each compression interval was 1 min and was repeated four times. Every rebound rate was calculated according to Eq. 6, and an average of the four rebound rates was obtained (hereinafter referred to as the average rebound rate). Five replicates were used and the average value was reported,

$$t_j = \frac{T_j - T_i/2}{T_i/2} \quad (6)$$

where t_j is the rebound rate, T_i is the sample thickness before the j^{th} compression (mm) (i = 0, 1, 2, 3), and T_j is the thickness of the sample after i^{th} compression (mm) (j = 1, 2, 3, 4).

Microstructure

The cell morphology and microstructure were observed using a scanning electron microscope (SEM) (FEI, Hillsboro, USA).

RESULTS AND DISCUSSION

Effect of Initial Water Content on Foaming Qualities

Figure 1 shows the porosity of the samples with different initial water contents. Similarly, Fig. 2 shows the average diameter of the bubbles with different initial water contents. Finally, Fig. 3 shows the standard deviation of the bubbles diameter distribution of the samples with different initial water contents.

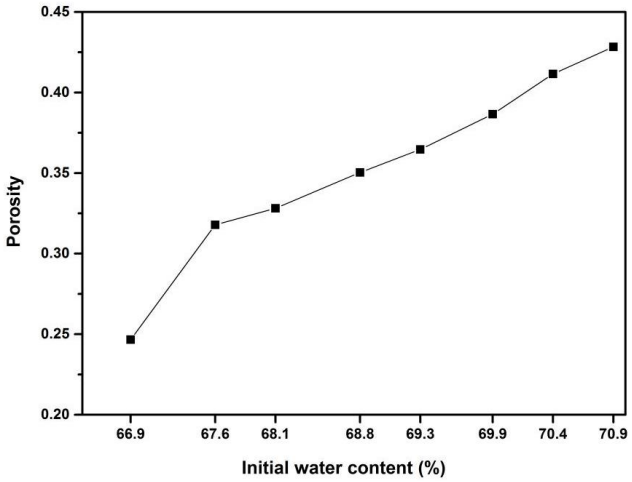

Fig. 1. Porosity of the samples with different initial water content

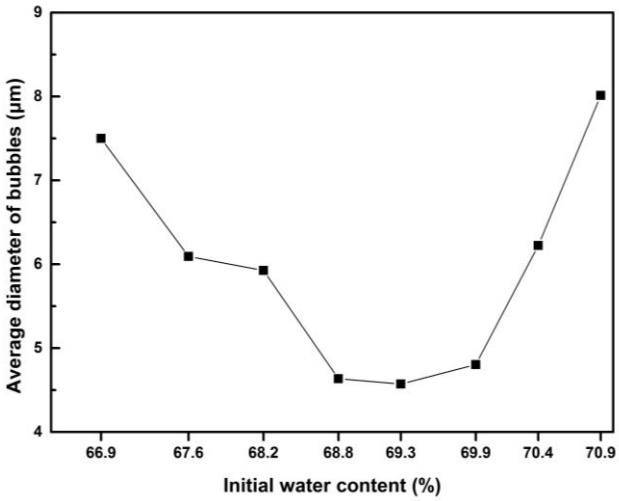

Fig. 2. Average diameter of bubbles with different initial water content

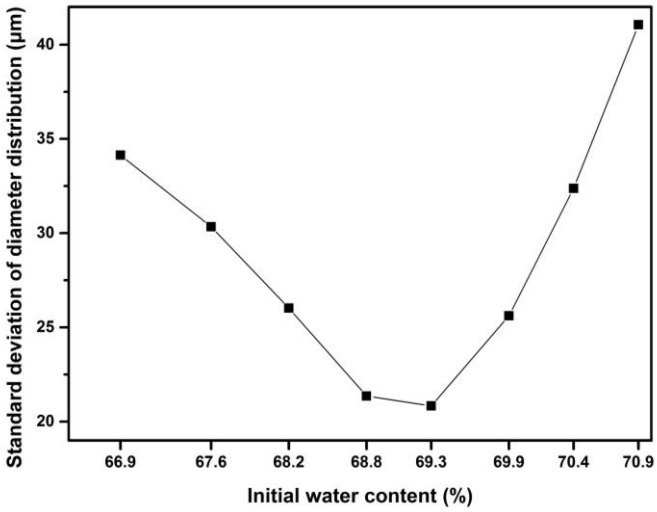

Fig. 3. Standard deviation of bubbles diameter distribution of the samples with different initial water content

Figure 1 shows that with the increase in the initial water content, the porosity of the samples increased gradually. Figures 2 and 3 show that with the increase in the initial water content, the average cell diameter and the standard deviation of the bubble diameter distribution decreased. When the initial water content was 69.3%, the sample average cell diameter and the standard deviation of the bubble diameter distribution reached their minimum. When the initial water content was greater than 69.3%, the sample average cell diameter and the standard deviation of bubble diameter distribution increased gradually.

A possible reason for this phenomenon was that when the initial water content was low, the initial embryo viscosity of the sample was great. This caused a large gas resistance in the sample forming process; thus the porosity of the sample was low. Furthermore, the average cell diameter and the standard deviation of the bubble diameter distribution were large; namely, the pore size had an uneven distribution. However, with the increase in the initial water content, the initial viscosity of the embryo decreased, which resulted in an easy bubble nucleation in the sample forming process and low gas resistance during the expansion process of the sample forming. This caused the porosity of the sample to increase, the average cell diameter and the standard deviation of bubble diameter distribution to decrease; as a consequence, the pore size distribution tended to be uniform. However, when the initial water content was too high, the initial viscosity of the embryo was low. This means small resistance of bubbles was required to be overcome during the expansion process, and the liquidity of the material became stronger in the forming process. Thus, the overflow phenomenon was produced and the gas spread more easily during the foaming process due to the low interfacial tension. This led to the gas not being captured well and even produced the phenomenon of consolidation or the rupture of bubbles. Eventually, the porosity, the average cell diameter, and the standard deviation of the bubble diameter distribution were all enlarged, namely, the pore size had an uneven distribution. In summary, when the initial water content was 69.3%, the initial embryo viscosity was most suitable for bubble growth and the porosity, pore size, and distribution of the sample were the best.

Effect of Initial Water Content on Mechanical Properties

Based on the static compression tests, the mechanical properties of the samples were acquired. Figure 4 shows the stress-strain curves of samples with different initial water contents. Figure 5 shows the cushioning coefficient stress curves of samples with different initial water contents. Figure 6 shows the average rebound rate of samples with different initial water contents.

As shown in Figs. 4, 5, and 6, the initial water content had a remarkable effect on the static compression and rebound properties of the samples. With the increase in initial water content, the stress-strain curves of the samples gradually moved downward, the minimum cushioning coefficient decreased, and the average rebound rate increased gradually.

When the initial water content was 69.3%, the stress-strain curve of the sample was the lowest, namely, the stress value that corresponded to the same strain was the lowest. The minimum cushioning coefficient of the sample reached the minimum, and the average rebound rate reached the maximum. When the initial water content was greater than 69.3%, the stress-strain curves of the samples moved upward. The minimum cushioning coefficient increased, and the average rebound rate gradually decreased.

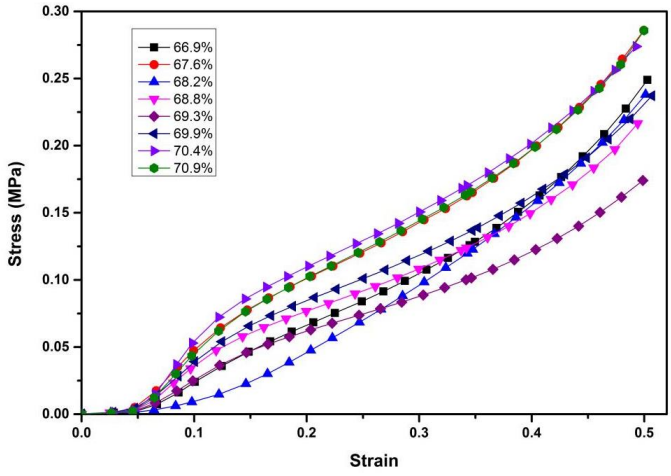

Fig. 4. Stress-strain curves of samples with different initial water contents

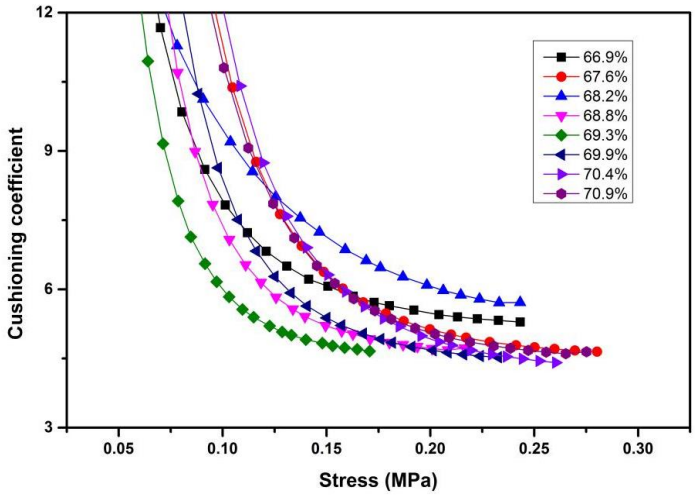

Fig. 5. Cushioning coefficient stress curves of samples with different initial water contents

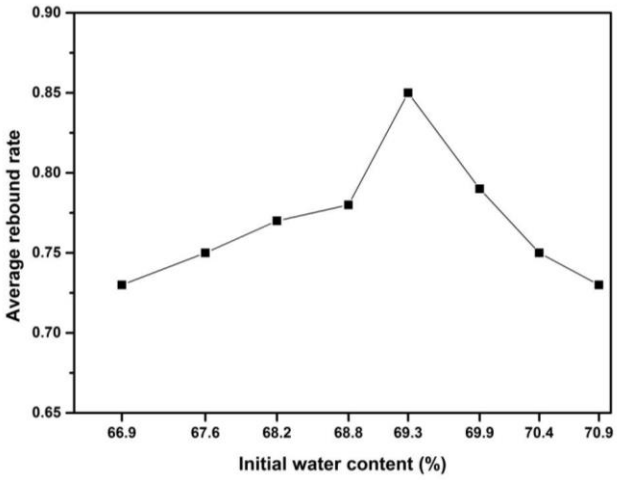

Fig. 6. Average rebound rate of samples with different initial water contents

A possible reason for this phenomenon was that when the initial water content was low, the initial embryo viscosity of the sample was high. This caused the tension inside the bubble to be smaller than outside the bubble in the sample forming process. Thus, the foaming quality was poor, the porosity of the sample was smaller, and the pore size had an uneven distribution. In the same strain condition, the stress was larger, the minimum buffer coefficient was larger, and the average rebound rate was lower. However, with the increase in the initial water content, the initial viscosity of the embryo decreased. This caused a decrease in the tension at the outside of the bubble in the sample forming process and increased porosity of the sample. In the same strain condition, the stress decreased, the minimum buffer coefficient decreased, and the average rebound rate increased. However, when the initial water content was greater than 69.3%, the initial viscosity of the embryo decreased. This led to smaller surface tension of the bubbles in the forming process, which was not enough to wrap the gas; thus the bubble burst and the bubble coalescence phenomenon occurred. This led to an increase in porosity and an uneven distribution in pore size. In the same strain condition, the stress was higher, the minimum buffer coefficient was higher, and the average rebound rate was lower. In summary, when the initial water content was 69.3%, the initial embryo viscosity was most suitable for bubble growth, and the porosity, pore size, and distribution of the sample were the optimal, which resulted in the best mechanical properties of the sample.

Foaming Mechanism of Plant Fiber Porous Cushioning Material

The plant fiber porous cushioning material was prepared by different forming processes with the homogeneous mixture of plant fiber, porous agent, adhesive, and other additives. As shown in Fig. 7, a three-dimensional mesh structure was formed by the overlapping of the wood powder and fiber. It shows that the function of the wood powder was to act as a skeleton, providing support. The fibers bonded with the wood powder by an adhesive, forming cell walls of the foam by bonding with other fibers. Due to the special raw materials of the plant fiber porous buffer material, there were big gaps between the fiber molecules, which was not conducive to the preservation of gas. However, its foaming mechanism was similar to the foaming mechanism of the polymer foaming material. The molding process was divided into four stages, namely, the

dissolution stage of the raw materials, the nucleation stage of the bubble, the growth stage of the bubble, and the stable solidification stage of the bubble hole.

During the dissolution process of the raw materials, the uniformity of the materials mixing was the precondition to ensure good foaming quality, due to it determining the distribution of the foaming agent, adhesive, and other components. In the nucleation stage of bubbles, if a large amount of bubble nucleation occurred with a uniform distribution in the embryo, high quality and uniform foam materials would be obtained (Xiao and Cao 2011). An out-phase nucleation mode was used in this experiment; namely, talcum powder was used as a nucleating agent and bubble nucleation was induced by nucleating sites that formed from the presence of the nucleating agent in the system. However, the bubble growth stage is a very complex dynamic process, which is affected by factors including the viscosity of embryo, bubble growth time, gas concentration, foaming temperature, *etc.* (Guo *et al*. 2012). Gas produced by the decomposition of the foaming agent in the embryo swelled gradually around the bubble nucleus, forming cells of the foam. The pore size and distribution of the bubble mainly depended on the viscosity of embryo.

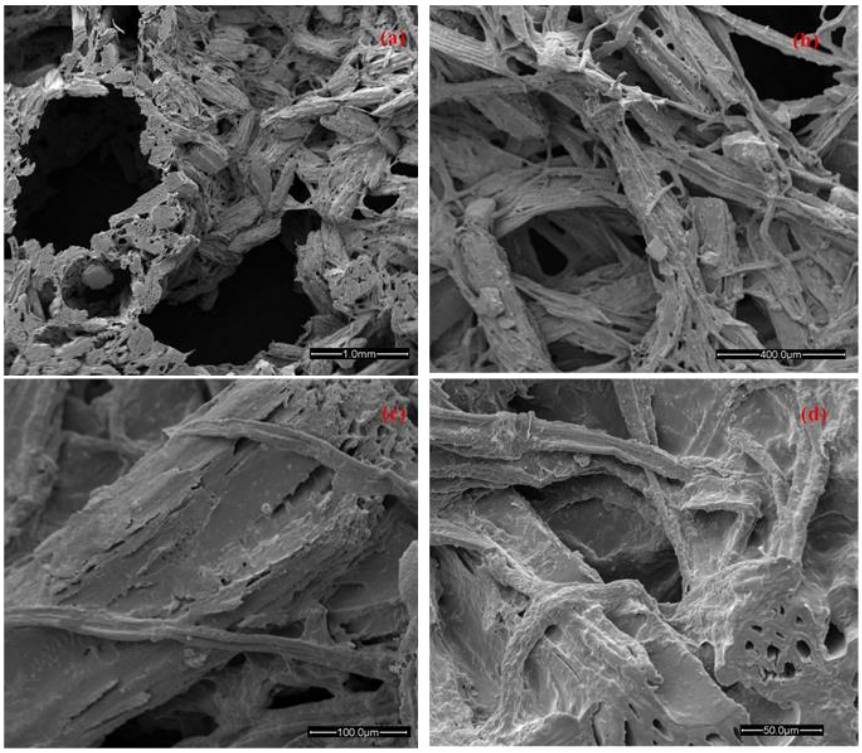

Fig. 7. SEM images of samples under different magnifications

According to the theory of bubble growth, the expansion power comes from the inner pressure of the cells and the expansion resistance comes from the viscoelastic properties of homogeneous mixture, external pressure, and surface tension. When the viscosity of the embryo is too large, the bubble expansion resistance is too large, which makes it difficult to trigger foaming. This results in decreased pore density, uneven pore size, and uneven distribution.

When the embryo viscosity is too low, the bubble expansion resistance is too small, which makes it impossible to support the expansion of bubbles. This causes the

merging and collapsing of bubbles. Therefore, proper viscosity of an embryo plays an extremely important role in the growth of the bubbles, because it is easier to make the porous buffer material with uniform pore size, distribution, and good mechanical properties (Liu *et al*. 2012).

In the stable solidification stage of the bubble hole, with the continuous evaporation of water in the embryo, the viscosity of the embryo increases and the foaming agent decomposes completely. The system tends to be stable and finally the bubble holes develop stable solidification.

CONCLUSIONS

1. When the initial water content was 69.3%, the initial embryo viscosity was most suitable for bubble growth, which resulted in the best porosity, pore size, and distribution of the plant fiber porous cushioning materials. The optimal mechanical properties of the cushioning materials could be obtained at this initial moisture content.
2. The foaming mechanism of the plant fiber porous cushioning material was similar to the foaming mechanism of a polymer foaming material.
3. The molding process was divided into four stages: the dissolution stage of raw materials, nucleation stage of bubble, growth stage of bubble, and stable solidification stage of bubble hole.
4. The embryo viscosity had the greatest influence on the bubble growth process.

ACKNOWLEDGEMENTS

The authors gratefully acknowledge financial support from the Harbin science and Technology Bureau outstanding subject leaders project (2016RAXXJ004) and the Fundamental Research Funds for Central Universities (2572016AB25) for this study.

REFERENCES CITED

Carr, L. G., Parra, D. F., Ponce, P., Lugão, A. B., and Buchler, P. M. (2006). "Influence of fibers on the mechanical properties of cassava starch foams," *Journal of Polymers and the Environment* 14(2), 179-183. DOI: 10.1007/s10924-006-0008-5

Cao, B. (2013). *Study on Preparation Process of Foam Wood Residual Fiber Cushion Packaging Material*, Master's Thesis, Northeast Forestry University, Harbin, China.

Chang, C. P., and Hung, S. C. (2003). "Manufacture of flame retardant foaming board from waste papers reinforced with phenol-formaldehyde resin," *Bioresource Technology* 86(2), 201-202. DOI: 10.1016/S0960-8524(02)00160-8

Chen, L.-K., Zhang, Q.-F., Lei, Z.-F., Wang, Y.-H., and Dong, X.-L. (2011). "Study on molding technology of straw fiber composite cushion material," *Packaging Engineering* 32(21), 11-14.

Fang, T. (2013). *Research on Properties of Cushioning Packaging Materials*, Master's Thesis, Tianjin University of Science and Technology, Tianjin, China.

Guo, A. -F., Li, J. F., Li, F. Y., and Lv, Y. (2012). "Research on the four-step foam forming mechanism of biomass materials," *Journal of Functional Materials* 1(43), 54-58.

Hong, H. J., Zhang, C., Yu, J., Luo, Z., He, L., and Wu, B. (2011). "Study on the influence of the viscosity to the microcellular structure of composites based on epoxy resin," *China Plastics Industry* 39(1), 85-87.

Huang, C. X., Zhu, Q., Li, C. C., Lin, W., and Xue, D. J. (2014). "Effects of micronized fibers on the cushion properties of foam buffer package materials," *BioResources* 9(4), 5940-5950. DOI: 10.15376/biores.9.4.5940-5950

GB/T 8168-2008 (2008). "Testing method of static compression for packaging cushioning materials," Standardization Administration of China, Beijing, China.

Ji, H. W., Guo, X., Guo, Y. H., and Wang, D. D. (2015). "Preparation and properties of bagasse cushioning material," *Journal of Functional Materials* 46(19), 19101-19105.

Lawton, J. W., Shogren, R. L., and Tiefenbacher, K. F. (2004). "Aspen fiber addition improves the mechanical properties of baked cornstarch foams," *Industrial Crops and Products* 19(1), 41-48. DOI: 10.1016/S0926-6690(03)00079-7

Li, G., Li, F. -Y., Guan, K. -K., Liu, P., Lv, Y., Jia, X. -J., and Li, J. -F. (2013). "Preparation and properties of biomass cushion packaging materials," *Journal of Functional Materials* 44(13), 1969-1971. DOI: 10.3969/j.issn.1001-9731.2013.13.036

Liu, X. -L., Lu, H. -J., and Xing, L. -Y. (2012). "Study on micro-morphology and structure control of bismaleimide foams," *Journal of Material Engineering* 2(8), 83-87. DOI: 10.3969/j.issn.1001-4381.2013.06.001

She, B. Y. (2007). *Study on Properties of Cushioning Material Made Plant Fiber with Network Structure*, Master's Thesis, Fujian Agricultural and Forestry University, Fuzhou, China.

Xiao, S. L. and Cao, B. (2011). "Dynamic research on foaming and interface of wood-plastic composite cushioning material for packaging," *Forest Engineering* 27(6), 54-57.

Wang, P., Liu, L., and Wei, Z. -Y. (2009). "Preparation and performance test of corn straw cushion packaging materials," *Packaging Engineering* 30(2), 16-18.

Wang, Y., Zhang, P., Gao, D., and Wang, B. T. (2012). "Effects of fiber content on the properties of PLA/corn straw fiber composite foamed material," *New Chemical Materials* 40(6), 79-81.

Wang, Z. (2012). *Foaming Properties and Model Research of Food Packaging Material Based on PLA/Corn Straw Fiber*, Master's Thesis, Zhejiang University, Hangzhou, China.

Zeng, G. -S., Lin, R. -Z., Zheng, L. -J., Chen, L., and Meng, C. (2013). "Comparation with performance of waste paper pulp reinforced starch-based foams with different foamer," *Journal of Functional Materials* 44(1), 51-55.

Zhao, D. F., Zhao, C. X., Ying, L. S., and Zhang, M. (2012). "Preparation and characterization of citrus pericarp residue/starch based biodegradable composite cushioning material," *Packaging Engineering* 33(21), 1-5.

Article submitted: January 19, 2017; Peer review completed: March 12, 2017; Revised version received and accepted: April 13, 2017; Published: April 28, 2017.
DOI: 10.15376/biores.12.2.4259-4269